How to cite: *Angew. Chem. Int. Ed.* **2022,** *61,* e202114792
International Edition: doi.org/10.1002/anie.202114792
German Edition: doi.org/10.1002/ange.202114792

Radicals | Hot Paper

A Persistent Phosphanyl-Substituted Thioketyl Radical Anion

*Lilian Sophie Szych, Yannic Pilopp, Jonas Bresien, Alexander Villinger, Jabor Rabeah, and Axel Schulz**

Dedicated to Professor Holger Braunschweig on the occasion of his 60th birthday

Abstract: *Alkali metal salts, M^+ [Ter(iPr)P–C(=S)–P(iPr)$_2$S]$^{\bullet-}$ (M = Na, K; **2_M**; Ter = 2,6-bis-(2,4,6-trimethylphenyl)phenyl) containing a room-temperature-stable thioketyl radical anion were obtained by reduction of the thioketone precursor, Ter(iPr)P–C(=S)–P(iPr)$_2$S (**1**), with alkali metals (Na, K). Single-crystal X-ray studies as well as EPR spectroscopy revealed the unequivocal existence of a thioketyl radical anion in the solid state and in solution, respectively. The computed Mulliken spin density within **2_M** is mainly located at the sulfur (49 %) and the carbonyl carbon (33 %) atoms. Upon adding [2.2.2]-cryptand to the radical species **2_K** to minimize the interionic interaction, an activation reaction was observed, yielding a potassium salt with a phosphanyl thioether based anion, [K(crypt)]$^+$ [Ter(iPr)P–C(–S-iPr)–P(iPr)$_2$S]$^-$ (**3**) as the product of an intermolecular shift of an iPr group from a second anion. The products were fully characterized and application of the radical anion as a reducing agent was demonstrated.*

Ever since the first syntheses of the benzophenone ketyl radical anion by Paul et al. and Schlenk et al. around 1900,[1–3] it has been known that (aromatic) ketones can react with alkali metals to form ketyl radicals. However, due to their high reactivity, it took almost 100 years before a benzophenone ketyl complex[4] and a solvent-free benzophenone radical anion[5] could be structurally characterized. Usually, ketyl radical anions are accessed by single electron transfer (SET) reductions using strong reductants such as elemental metals.[6–11] Today, ketyl radicals are widely used, e.g. as ligands in coordination chemistry,[4,12–20] in C–C bond-formation reactions,[21] as reductants,[22] and for the dehydration and deoxygenation of solvents.[23] Depending on the substitution pattern of ketyl radicals, the spin density distribution may vary. While the spin density in the benzophenone radical anion [Ph$_2$CO]$^{\bullet-}$ is located on the phenyl rings (56 %), on the oxygen atom (23 %) and on the carbonyl carbon atom (20 %),[5,24] in species without electron-delocalizing substituents such as e.g., [(*t*Bu$_2$MeSi)$_2$CO]$^{\bullet-}$, the spin density is mainly located at the carbonyl carbon atom.[24] Thioketones, and related species[25–29] like dithioesters,[30–32] are known to be good spin-trapping reagents for carbon-centered,[33–36] organometallic[33,36,37] and phosphorus-centered[38] radicals. Their common reaction mechanism involves adduct formation yielding different radical intermediates. Thioketyl radicals are most commonly generated by SET reductions either electrochemically,[39,40] photochemically,[41–44] or by using metal-based reductants.[45–48] Due to their sensitivity, a full characterization of thioketyls is difficult and in the past, these species have often only been synthesized in situ, for example in EPR studies or for their usage in polymerization processes.[45] To the best of our knowledge, no examples of detailed structural investigations on thioketyl radical anions are known to date. We recently isolated a phosphanyl-stabilized thioketone (**1**, Scheme 1).[49] In this work it is shown that reduction of **1** with an alkali metal gives a stable phosphanyl thioketyl radical (**2_M**). Herein, we present the detailed characterization of the isolated radical species **2_M** in solution and in the solid state as well as first reactivity investigations.

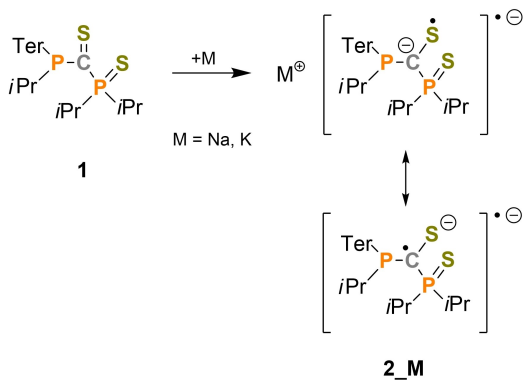

Scheme 1. Synthesis of the thioketyl radical anion containing salts **2_K** and **2_Na** via conversion of **1** with elemental Na or K metal (or with KC_8). The unpaired electron is delocalized along the C–S moiety as shown by the two resonance formulae. In all Lewis formulae, the lone pairs are omitted for clarity.

[*] L. S. Szych, Y. Pilopp, Dr. J. Bresien, Dr. A. Villinger, Prof. Dr. A. Schulz
Institut für Chemie, Universität Rostock
Albert-Einstein-Straße 3a, 18059 Rostock (Germany)
E-mail: axel.schulz@uni-rostock.de
Dr. J. Rabeah, Prof. Dr. A. Schulz
Leibniz-Institut für Katalyse e.V. an der Universität Rostock
Albert-Einstein-Straße 29a, 18059 Rostock (Germany)

The synthesis of the alkali metal salts of the new thioketyl radical anion begins with the preparation of thioketone **1** (see Supporting Information),[49] bearing two sterically demanding phosphanyl substituents (due to the attached *i*Pr and Ter moieties; Ter = terphenyl = 2,6-bis-(2,4,6-trimethylphenyl)phenyl[50]). The radical species **2_K** and **2_Na** were obtained in a SET reduction process of the starting material **1** in THF at room temperature, using either KC_8 as reductant, or elemental sodium or potassium in form of a "metal mirror" in a flask (Scheme 1). The reduction process can be easily traced by observing the color change of the reaction solution from deep green to an intense red (both for **2_Na** and **2_K**). However, while reduction with elemental Na takes about an hour, reduction with K is complete in a few minutes. Also, ^{31}P NMR spectroscopy is well suited to follow the course of the reaction since the signals of both P atoms of **1** disappear upon reduction. After workup, the radical species **2_K** and **2_Na** were obtained in good yields (81 % and 64 %). Crystallization of **2_K** from a mixture of THF/benzene gave small orange single crystals of rather poor quality which, however, still allowed a refinement of the data (see Supporting Information). A comparison of structural parameters of **2_K** and the starting material **1** can be found in Table 1.

Table 1: Selected structural parameters of **1**, **2_K** and **3** (vide infra) in the single crystal.

Parameter[a]	**1**[b]	**2_K**	**3**
C1–S1	1.658(1)	1.705(6)	1.766(2)
P2–S2	1.9537(4)	1.994(8)	2.0123(7)
C1–P1	1.764(1)	1.809(7)	1.772(2)
C1–P2	1.855(1)	1.786(8)	1.750(2)
P1–C1–S1	121.67(6)	125.3(4)	126.7(1)
da1[c]	−162.2(1)	−170.1(7)	171.5(2)

[a] Bond lengths in Ångstrom [Å] and angles in degree [°]. [b] Data taken from Ref. [49]. [c] da1 = ∢ (P1–C1–S1–P2) dihedral angle.

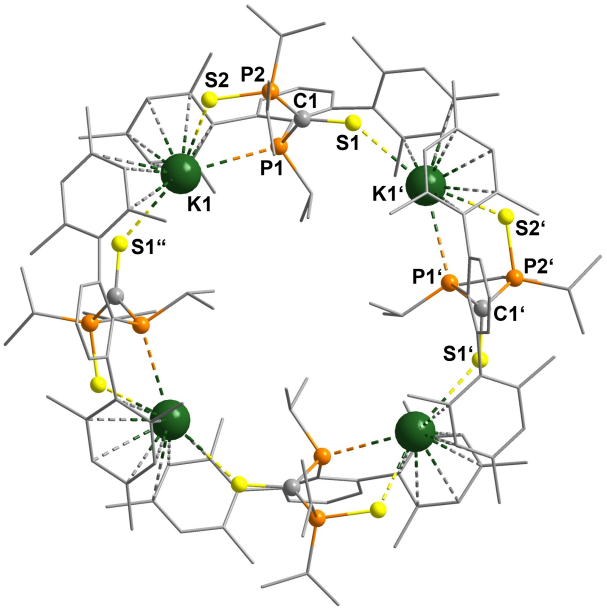

Figure 1. Molecular structure of tetramer of **2_K** in the single crystal. Only the major component (A-layer, 64 %) is depicted for clarity. H atoms omitted for clarity. An ORTEP representation of the monomeric unit of **2_K** can be found in the Supporting Information, Figure S1.

2_K crystallizes in the tetragonal space group $I4_1/acd$ with 32 formula units per unit cell. There are three types of different interionic interactions (Figure 1): The K1 cation is coordinated to the P1 atom (K1···P1 3.336(3) Å; Σr_{cov}(K–P): 3.07 Å;[51] Σr_{vdW}(K···P): 4.55 Å)[52] and also to S2 atom (K1···S2 3.075(3) Å; Σr_{cov}(K–S): 2.99 Å;[51] Σr_{vdW}(K···S): 4.55 Å).[52] Additionally, the K1 cation is coordinated by the S1″ atom of a neighboring molecule of **2_K** (S1″···K1 3.128(3) Å) resulting in a tetrameric arrangement in the single crystal. Further coordination of the K1 cation occurs via the Mes-group of the Ter-substituent (η^6 fashion, average distance C···K1 3.2 Å; Σr_{vdW}(K···C): 4.45 Å),[52] which is a common structural phenomenon in Ter-stabilized potassium phosphides.[49] In addition, further intermolecular coordination also occurs via a second adjacent Mes substituent (η^3 fashion, average distance C···K1 3.4 Å). Therefore, in the tetramer, the four Ter-substituents are arranged alternately, with one Ter substituent coordinating two K ions from below and the adjacent Ter-substituent coordinating two K ions from above, thus forming a Ter pocket in which the potassium ion is embedded. The thioketyl radical anion, which is coordinated by two adjacent potassium ions, features a slightly bent P–C(S)–P–S core with deviation from planarity between 7 and 18°. The most prominent structural feature, the C1–S1 bond length of 1.705(6) Å, ranges between a single and a double bond (Σr_{cov}(C–S): 1.78 Å; (Σr_{cov}(C=S): 1.61 Å)[51]) and is therefore significantly longer than the corresponding double bond in the starting material **1** (cf. 1.658(1) Å, Table 1).[49] This bond elongation can be attributed to the population of the antibonding π* orbital with one electron in **2_K** (see IR spectra of **1** and **2_K**, Figure S6; as well as Figure S7) and has been reported for analogous ketyl derivatives before.[5,11] This structural change of the C–S bond upon reduction is also manifested in the IR spectrum. Starting material **1** exhibits a C–S stretching band in its IR spectrum at 983 cm^{-1}, which is shifted to lower wave numbers of 672 cm^{-1} (**2_K**) or 670 cm^{-1} (**2_Na**) in the radical compounds. This observation is in good accordance with the findings from experimental and theoretical investigations on benzophenone and its radical anion by Frenette and Juneau.[11] The shift can be explained, analogously to the elongation of the C=S bond in the single crystal of **2_K** (vide supra), by the population of the antibonding π* orbital with one electron in **2_K** and **2_Na** (formally lowest unoccupied molecular orbital LUMO in **1** becomes singly occupied molecular orbital SOMO in **2**), which decreases the effective C–S bond order (see Supporting Information Figure S7).

To further study the reduction process, EPR spectra and a cyclic voltammogram (CV) were recorded. The CV of the starting material **1** in THF solution (Figure 2, right) nicely shows the reversible reduction process of **1** to **2**$^{\bullet-}$. The cathodic peak potential of **1** was estimated to be E_{pc} = −1.71 V and E_{pa} = −1.57 V for the anodic peak potential. The EPR spectra of **2_K** and **2_Na** in benzene solution

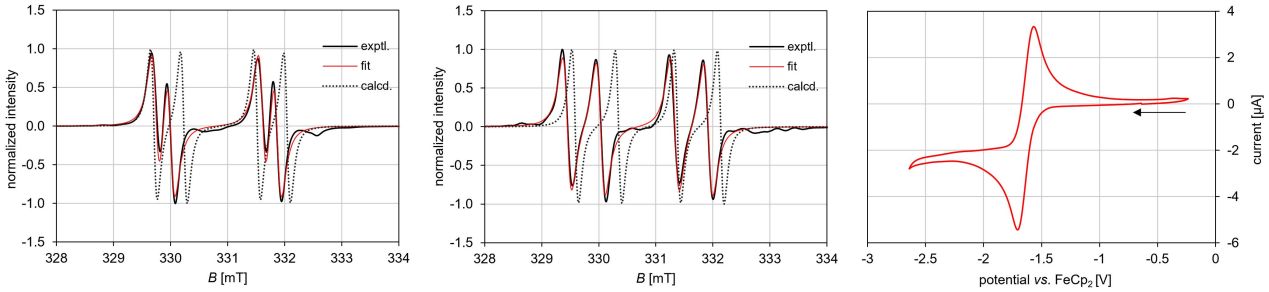

Figure 2. Left: Experimental (black), simulated (red) and calculated (dotted) EPR spectra of **2_K** in C_6D_6 (0.60 mg mL^{-1}) at 301 K.[53–67] Middle: Experimental (black), simulated (red) and calculated (dotted) EPR spectra of **2_Na** in C_6D_6 (0.38 mg mL^{-1}) at 291 K. Right: Cyclic voltammogram of 0.01 M solution of **1** in THF at glassy carbon electrode; [N^{n}Bu$_4$][PF$_6$] as electrolyte, formal redox potentials are referred to the $[FeCp_2]/[FeCp_2]^+$ couple, scan rate 50 mV s^{-1}.

confirm their radical nature and show a doublet of doublets consistent with hyperfine coupling to the two phosphorus atoms P1 and P2. The agreement between experimental and calculated *g* values and hyperfine coupling constants is reasonable (Figure 2 and Table 2). In contrast, the EPR spectra of **2_K** and **2_Na** in THF solution (see Supporting Information, Figure S8) indicate the presence of different dynamic conformers and/or coordination patterns of cation and anion upon changing the solvent (see Supporting Information, section 4.2). This is comparable to the results of Raman spectroscopic investigations by Frenette and Juneau revealing that the benzophenone ketyl system in THF solution is "best described as a combination of bound and unbound" counterion.[11] The observation of the rather complex EPR spectrum of **2_K** in THF and the idea of bound and unbound radical anion species prompted us to investigate a situation where the "naked" radical anion is present in solution.

Therefore, we added [2.2.2]-cryptand (=crypt= 4,7,13,16,21,24-hexaoxa-1,10-diazabicyclo[8.8.8]hexacosane) to the radical (**2_K**) to complex the K counterion and thus prevent the cation from interacting with the radical anion. After adding an equimolar amount of cryptand to a freshly prepared solution of **2_K** in THF, the sample shows two broad doublets in its EPR spectrum (see Supporting Information, Figure S9). These doublets can be attributed to two conformers of the "naked" radical anion **2**$^{\bullet-}$. The coordination of the metal counterion to the radical anion in **2_K** and in **2_Na** in non-polar solvents (such as benzene) probably results in a rigid, stable conformation of cation-anion-pairs in solution. When the cation is coordinated by the cryptand (after addition), the "naked" radical anion **2**$^{\bullet-}$ is no longer stabilized in the rigid conformation but is significantly more flexible, enabling the formation of different conformers of the radical anion in solution.

Attempts to crystallize **2_K**[crypt] were not successful but resulted in the formation of an intermolecular activation product, which was obtained after a week of storage in solution in the form of a few, yellowish single crystals. Single-crystal structure elucidation unequivocally revealed the formation of the phosphanyl thioether **3** in a yet unknown process (Scheme 2, Figure 4). In **3**, an additional *i*Pr group is attached to the S1 atom, which is probably the result of an intermolecular activation reaction. Other potential reaction products of this reaction could not be identified. The intermolecular reaction of **2_K** could neither be observed in a solution of pure **2_K** in THF nor in benzene. This indicates that the coordination of the K^+ ion by the cryptand increases the reactivity of the radical anion, as a result of the loss of stabilization by coordination to its counterion. Hence, the observed reactivity of **2_K**[crypt] is in good accordance with the observed findings of the EPR investigations. As expected, the ^{31}P NMR spectrum of **3** shows two doublets at 17.1 ppm and 71.7 ppm ($^2J(^{31}P, ^{31}P)$ = 200 Hz).

The observed addition of the *i*Pr group to the S1 atom (Scheme 2, Figure 4) is in good accordance with calculations of the spin density distribution in the radical species **2_M**. The Mulliken spin density in the radical species is mainly located at the S atoms (**2_K**: S1 0.488; **2_Na**: S1 0.495) and at the carbonyl C1 atoms (**2_K**: C1 0.333; **2_Na**: C1 0.331,

Table 2: Experimental and computed EPR parameters (in brackets) of the compounds **2_K** (0.60 mg mL^{-1}, 301 K) and **2_Na** (0.38 mg mL^{-1}, 291 K) in benzene solution. The experimental data are taken from the fitted spectra.

Compound	g_{iso}	A^1_{iso}(^{31}P2) [MHz]	A^2_{iso}(^{31}P1) [MHz]
2_K	2.0149	−52.5	−7.5
	[2.0145]	[−51.0]	[−14.8]
2_Na	2.0156	−53.3	−16.5
	[2.0146]	[−50.5]	[−21.5]

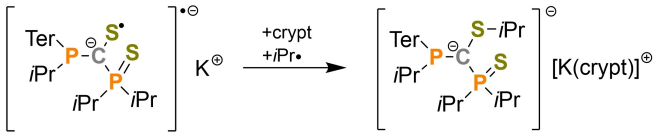

2_K **3**

Scheme 2. Intermolecular activation reaction of **2_K** with *i*Pr radical (from a second molecule **2_K**) upon longer storage with equimolar amount of cryptand in solution, yielding the product **3**. Other reaction products of this intermolecular activation reaction could not be identified.

Figure 3). Only a rather low spin density is found at both P atoms (**2_K**: P1 0.034, P2: 0.028; **2_Na**: P1 0.033 P2: 0.028, Figure 3) of **2_K** and **2_Na**, so that it is certainly justifiable to speak of a thioketyl (carbon/sulfur)-centered radical. Therefore, it is not surprising that the *i*Pr group migrates to the sulfur, since the largest amount of spin density is located there.

Conversion of the radical anion of **2_K** with different substrates indicated that **2_K** does react as a one-electron reducing reagent forming **1** as the main reaction product (see Supporting Information, section 3.4, for further details).

Finally, a short word on the structure of **3**, which crystallizes in the orthorhombic space group $Pna2_1$ with four formula units per unit cell (Figure 4). In the crystal, well separated ion pairs of $[K(crypt)]^+[Ter(iPr)P–C(S\text{-}iPr)\text{-}P(S)iPr_2]^-$ with no significant cation-anion interactions are found, in contrast to the structure of **2_K**. As expected, the K1 ion in **3** is coordinated by the [2.2.2]-cryptand in a "pocket" formed by the O atoms (average O···K distance: 2.81 Å; Σr_{vdW}(O···K): 4.27 Å) and the N atoms (average N···K distance: 3.05 Å; Σr_{vdW}(N···K): 4.30 Å) of the cryptand. Within the molecular anion of **3**, the P1–C1 bond length of 1.773(2) Å as well as the P2–C1 bond length of 1.750(2) Å range between the sum of the covalent radii for a corresponding single and double bond (Σr_{cov}(P–C): 1.86 Å; Σr_{cov}(P=C): 1.69 Å).[51] The C1–S1 bond length of 1.766(2) Å is in the range of a single bond (Σr_{cov}(C–S): 1.78 Å), and significantly longer than the corresponding bond in **2_K** (Table 1).[68]

In summary, salts bearing a stable phosphanylthioketyl radical anion were synthesized by reduction of a phosphanylthioketone with elemental sodium or potassium. The radical character was studied by EPR and CV experiments, clearly indicating the presence of a thioketyl radical anion. Calculations revealed that the spin density in **2_M** is mainly localized at the thiocarbonyl C–S moiety. The CV measurement indicates that the reduction of the phosphanylthioketone **1** is a reversible process. The high reduction potential of the stable radical **2_K** was demonstrated experimentally by the reaction with small molecules.

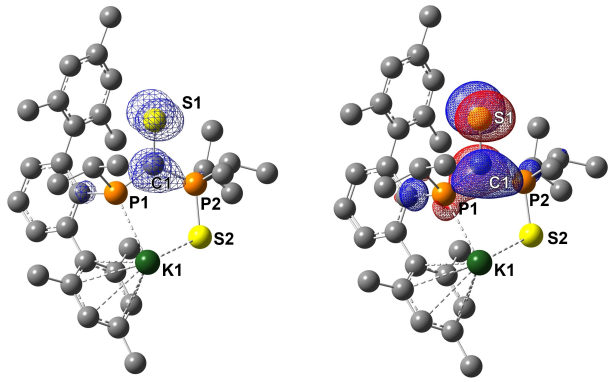

Figure 3. Left: Plot[65] of the spin density of **2_K** (isosurfaces set at 0.004 a.u.). Right: SOMO of **2_K** (isosurfaces set at 0.04 a.u). Optimization of structures/calculations at the PBE-D3/def2-TZVP level of theory in the gas phase. Hydrogen atoms omitted for clarity.

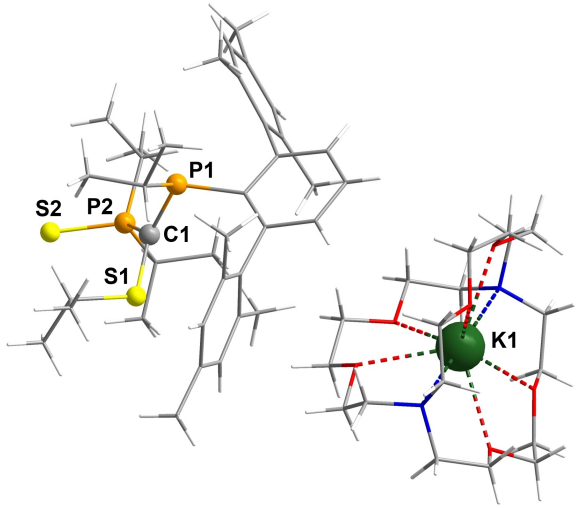

Figure 4. Molecular structure of **3** in the single crystal. Blue = nitrogen, red = oxygen, white = hydrogen.

Acknowledgements

L.S.S. wishes to thank the Fonds der chemischen Industrie and the Studienstiftung des deutschen Volkes for financial support. The University of Rostock and especially M. Willert are acknowledged for access to the cluster computer and support with software installations. We would like to thank J.-E. Siewert for assisting with the CV measurements and Dr. C. Hering-Junghans for the kind donation of [2.2.2]-cryptand. Dr. R. Wustrack is acknowledged for his help with reviewing literature. Open Access funding enabled and organized by Projekt DEAL.

Conflict of Interest

The authors declare no conflict of interest.

Data Availability Statement

The data that support the findings of this study are available in the Supporting Information of this article.

Keywords: Ketyl · Phosphorus · Radicals · Sulfur · Synthesis

[1] E. Beckmann, T. Paul, *Justus Liebigs Ann. Chem.* **1891**, *266*, 1–28.
[2] W. Schlenk, T. Weickel, *Ber. Dtsch. Chem. Ges.* **1911**, *44*, 1182–1189.
[3] W. Schlenk, A. Thal, *Ber. Dtsch. Chem. Ges.* **1913**, *46*, 2840–2854.
[4] Z. Hou, X. Jia, M. Hoshino, Y. Wakatsuki, *Angew. Chem. Int. Ed. Engl.* **1997**, *36*, 1292–1294; *Angew. Chem.* **1997**, *109*, 1348–1350.

[5] T. A. Scott, B. A. Ooro, D. J. Collins, M. Shatruk, A. Yakovenko, K. R. Dunbar, H.-C. Zhou, *Chem. Commun.* **2009**, 65–67.
[6] G. Nocera, A. Young, F. Palumbo, K. J. Emery, G. Coulthard, T. McGuire, T. Tuttle, J. A. Murphy, *J. Am. Chem. Soc.* **2018**, *140*, 9751–9757.
[7] Y. Yamamoto, R. Hattori, T. Miwa, Y. Nakagai, T. Kubota, C. Yamamoto, Y. Okamoto, K. Itoh, *J. Org. Chem.* **2001**, *66*, 3865–3870.
[8] A. Fürstner, N. Shi, *J. Am. Chem. Soc.* **1996**, *118*, 2533–2534.
[9] P. Bichovski, T. M. Haas, D. Kratzert, J. Streuff, *Chem. Eur. J.* **2015**, *21*, 2339–2342.
[10] L. P. T. Hong, C. Chak, C. D. Donner, *Org. Biomol. Chem.* **2013**, *11*, 6186–6194.
[11] A. Juneau, M. Frenette, *J. Phys. Chem. B* **2021**, *125*, 1595–1603.
[12] Z. Hou, X. Jia, A. Fujita, H. Tezuka, H. Yamazaki, Y. Wakatsuki, *Chem. Eur. J.* **2000**, *6*, 2994–3005.
[13] Z. Hou, A. Fujita, Y. Zhang, T. Miyano, H. Yamazaki, Y. Wakatsuki, *J. Am. Chem. Soc.* **1998**, *120*, 754–766.
[14] R. H. Heyn, T. D. Tilley, *Inorg. Chim. Acta* **2002**, *341*, 91–98.
[15] I. Lopes, R. Dias, Â. Domingos, N. Marques, *J. Alloys Compd.* **2002**, *344*, 60–64.
[16] O. P. Lam, C. Anthon, F. W. Heinemann, J. M. O'Connor, K. Meyer, *J. Am. Chem. Soc.* **2008**, *130*, 6567–6576.
[17] Â. Domingos, I. Lopes, J. C. Waerenborgh, N. Marques, G. Y. Lin, X. W. Zhang, J. Takats, R. McDonald, A. C. Hillier, A. Sella, M. R. J. Elsegood, V. W. Day, *Inorg. Chem.* **2007**, *46*, 9415–9424.
[18] S. L. Marquard, M. W. Bezpalko, B. M. Foxman, C. M. Thomas, *J. Am. Chem. Soc.* **2013**, *135*, 6018–6021.
[19] C. Jones, L. McDyre, D. M. Murphy, A. Stasch, *Chem. Commun.* **2010**, *46*, 1511–1513.
[20] E. M. Matson, J. J. Kiernicki, N. H. Anderson, P. E. Fanwick, S. C. Bart, *Dalton Trans.* **2014**, *43*, 17885–17888.
[21] Á. Péter, S. Agasti, O. Knowles, E. Pye, D. J. Procter, *Chem. Soc. Rev.* **2021**, *50*, 5349–5365.
[22] N. G. Connelly, W. E. Geiger, *Chem. Rev.* **1996**, *96*, 877–910.
[23] W. L. F. Armarego, C. L. L. Chai, *Purification of Laboratory Chemicals*, Elsevier, Amsterdam, **2013**.
[24] Y. Kratish, D. Pinchuk, A. Kaushansky, V. Molev, B. Tumanskii, D. Bravo-Zhivotovskii, Y. Apeloig, *Angew. Chem. Int. Ed.* **2019**, *58*, 18849–18853; *Angew. Chem.* **2019**, *131*, 19025–19029.
[25] H. Bock, P. Hänel, H.-F. Herrmann, H. torn Dieck, *Z. Naturforsch. B* **1988**, *43*, 1240–1246.
[26] Y. Wang, Y. Xie, P. Wei, S. A. Blair, D. Cui, M. K. Johnson, H. F. Schaefer, G. H. Robinson, *J. Am. Chem. Soc.* **2020**, *142*, 17301–17305.
[27] D. Casarini, L. Lunazzi, G. Placucci, T. Ishida, A. Ishii, R. Okazaki, *J. Org. Chem.* **1988**, *53*, 1582–1584.
[28] A. Alberti, M. Benaglia, M. Guerra, M. Gulea, D. Macciantelli, S. Masson, *Org. Lett.* **2008**, *10*, 3327–3330.
[29] Y. Wang, H. P. Hickox, Y. Xie, P. Wei, S. A. Blair, M. K. Johnson, H. F. Schaefer, G. H. Robinson, *J. Am. Chem. Soc.* **2017**, *139*, 6859–6862.
[30] A. Alberti, M. Benaglia, M. Laus, K. Sparnacci, *J. Org. Chem.* **2002**, *67*, 7911–7914.
[31] J. Voss, D. Buddensiek, J. F. Rosenboom, *Phosphorus Sulfur Silicon Relat. Elem.* **2012**, *187*, 382–391.
[32] R. Borghi, M. A. Cremonini, L. Lunazzi, G. Placucci, *J. Org. Chem.* **1994**, *59*, 3726–3729.
[33] J. C. Scaiano, K. U. Ingold, *J. Am. Chem. Soc.* **1976**, *98*, 4727–4732.
[34] A. Alberti, B. F. Bonini, G. F. Pedulli, *Tetrahedron Lett.* **1987**, *28*, 3737–3740.
[35] A. Alberti, M. Benaglia, B. F. Bonini, G. F. Pedulli, *J. Chem. Soc. Faraday Trans. 1* **1988**, *84*, 3347–3358.
[36] A. Alberti, M. Guerra, P. Hapiot, T. Lequeux, D. Macciantelli, S. Masson, *Phys. Chem. Chem. Phys.* **2005**, *7*, 250–257.
[37] B. B. Adeleke, K. S. Chen, J. K. S. Wan, *J. Organomet. Chem.* **1981**, *208*, 317–326.
[38] W. G. McGimpsey, M. C. Depew, J. K. S. Wan, *Phosphorus Sulfur Relat. Elem.* **1984**, *21*, 135–144.
[39] C.-P. Klages, J. Voß, *Chem. Ber.* **1980**, *113*, 2255–2277.
[40] C.-P. Klages, J. Voss, *Angew. Chem. Int. Ed. Engl.* **1977**, *16*, 726–727; *Angew. Chem.* **1977**, *89*, 744–745.
[41] G. N. R. Tripathi, D. M. Chipman, R. H. Schuler, D. A. Armstrong, *J. Phys. Chem.* **1995**, *99*, 5264–5268.
[42] D. A. Armstrong, Q. Sun, R. H. Schuler, *J. Phys. Chem.* **1996**, *100*, 9892–9899.
[43] N. Kito, A. Ohno, *Bull. Chem. Soc. Jpn.* **1973**, *46*, 2487–2489.
[44] A. G. Davies, A. G. Neville, *J. Chem. Soc. Perkin Trans. 2* **1992**, 171–173.
[45] Y. Minoura, S. Tsubio, *J. Polym. Sci. Part A* **1970**, *8*, 125–138.
[46] Y. Minoura, S. Tsuboi, *J. Org. Chem.* **1972**, *37*, 2064–2069.
[47] D. Buddensiek, B. Köpke, J. Voß, *Chem. Ber.* **1987**, *120*, 575–581.
[48] A. Alberti, M. Benaglia, D. Macciantelli, M. Marcaccio, A. Olmeda, G. F. Pedulli, S. Roffia, *J. Org. Chem.* **1997**, *62*, 6309–6315.
[49] J. Bresien, Y. Pilopp, A. Schulz, L. S. Szych, A. Villinger, R. Wustrack, *Inorg. Chem.* **2020**, *59*, 13561–13571.
[50] S. Demeshko, C. Godemann, R. Kuzora, A. Schulz, A. Villinger, *Angew. Chem. Int. Ed.* **2013**, *52*, 2105–2108; *Angew. Chem.* **2013**, *125*, 2159–2162.
[51] P. Pyykkö, M. Atsumi, *Chem. Eur. J.* **2009**, *15*, 12770–12779.
[52] M. Mantina, A. C. Chamberlin, R. Valero, C. J. Cramer, D. G. Truhlar, *J. Phys. Chem. A* **2009**, *113*, 5806–5812.
[53] F. Neese, *J. Chem. Phys.* **2001**, *115*, 11080–11096.
[54] F. Neese, *J. Chem. Phys.* **2003**, *118*, 3939–3948.
[55] F. Neese, *J. Chem. Phys.* **2005**, *122*, 034107.
[56] F. Neese in *EMagRes* (Eds.: R. K. Harris, R. L. Wasylishen), Wiley, Chichester, **2017**, pp. 1–22.
[57] B. A. Heß, C. M. Marian, U. Wahlgren, O. Gropen, *Chem. Phys. Lett.* **1996**, *251*, 365–371.
[58] J. P. Perdew, K. Burke, M. Ernzerhof, *Phys. Rev. Lett.* **1996**, *77*, 3865–3868.
[59] J. P. Perdew, K. Burke, M. Ernzerhof, *Phys. Rev. Lett.* **1997**, *78*, 1396–1396.
[60] C. Adamo, V. Barone, *J. Chem. Phys.* **1999**, *110*, 6158–6170.
[61] F. Neese, F. Wennmohs, A. Hansen, U. Becker, *Chem. Phys.* **2009**, *356*, 98–109.
[62] S. Stoll, A. Schweiger, *J. Magn. Reson.* **2006**, *178*, 42–55.
[63] S. Stoll, R. D. Britt, *Phys. Chem. Chem. Phys.* **2009**, *11*, 6614–6625.
[64] S. Stoll in *Multifrequency Electron Paramagnetic Resonance* (Ed.: S. K. Misra), Wiley-VCH, Weinheim, **2014**, pp. 69–138.
[65] T. Lu, F. Chen, *J. Comput. Chem.* **2012**, *33*, 580–592.
[66] F. Neese, *WIREs Comput. Mol. Sci.* **2018**, *8*, e1327.
[67] F. Neese, F. Wennmohs, U. Becker, C. Riplinger, *J. Chem. Phys.* **2020**, *152*, 224108.
[68] Deposition Numbers 2122867 (for **2_K**) and 2114487 (for **3**) contain the supplementary crystallographic data for this paper. These data are provided free of charge by the joint Cambridge Crystallographic Data Centre and Fachinformationszentrum Karlsruhe Access Structures service www.ccdc.cam.ac.uk/structures.

Manuscript received: November 1, 2021
Accepted manuscript online: November 29, 2021
Version of record online: January 12, 2022